Using the proxy cablecal: geodetic impact at GGAO12M

A. E. Niell

2023/08/04

Introduction/summary

The goal of this study is to investigate the impact of rapid quasi-periodic variations in the proxy cablecal (pcmt) delay on the geodetic parameter estimation, as seen at GGAO12M. Imprecise modeling of the time variation of the pcmt delay increases the unmodeled noise of the estimation process and thus affects the parameter uncertainties of the geodetic results. This is important because ignoring the proxy cablecal correction affects the estimated position of the antenna at a level of many millimeters.

1. The importance and use of phasecal and cablecal for VGOS

Two critical components of the geodetic VLBI system are the phase calibration signals (phasecal) and the reference frequency cable measurement device (historically known as cablecal). The phasecal is used to align the phases across each band, which corrects for phase variations introduced by the electronics. The cablecal is used to remove delays introduced by the reference frequency cable that are related to the orientation of the antenna.

The delay within the antenna system experienced by the phasecal consists of the delay from the source of the reference frequency up to the phasecal injection point and and the delay from there down through the electronics to the digitizer. Ideally, a cable delay measurement device is used to correct for variation in the first segment, i.e. for changes in the electrical path of the reference frequency signal that is provided to the phasecal generator. This part of the delay is not experienced by the astronomical signal but is part of the observed VLBI delay between the antennas, so it should be removed for the geodetic analysis.

Perhaps the most important function of the cablecal for geodesy is to remove delays introduced by the reference frequency cable that are related to the orientation of the antenna. The differences in value, which can reach many tens of picoseconds, are usually attributable to bending and/or twisting of the cable as the antenna moves. The cable delay at any antenna position is a function of both the orientation of the antenna and the direction of motion getting there (hysteresis). (See Figures 1 and 2 for examples.) A systematic and repeatable change with orientation, such as more delay at low elevations or more delay in the north-south than in the east-west direction, if not corrected, would be calculated in the geodetic estimation process as apparent displacements of the antenna in the local vertical or horizontal position, respectively.

For an antenna with a functioning cable delay measurement system (CDMS, which can be either the hardware cable calibrator ((Rogers, 2015); Garcia-Carreña et al (2022)) or the newer Software Defined Radio (SDR) version (Vierinen and Beaudoin, (2014), Ruszczyk et al (2023)), the delay values are recorded either in the log file or in a separate file and applied in the geodetic analysis. However, some antennas have not been provided with a CDMS, and on occasion a CDMS fails to operate properly. In those circumstances the cable delay must be obtained by some alternative method in order to avoid an error in the estimated position of the antenna (described in the next section).

2. The proxy cable delay measurement as a substitute for the hardware cable delay measurement system

The phase of each phasecal tone is delayed by the electrical path length from the origin of the reference frequency generator, which for VGOS antennas is the 5-MHz distributor attached to the Hydrogen maser frequency standard, to the point where it is digitized and time-tagged. The delay calculated from the phasecal tones within all frequency channels within a band is designated the proxy cablecal delay. Due to its origin, the delay is also referred to as the phasecal multitone delay, or pcmt delay, or simply pcmt, although it is not directly related to, nor derivable from, the multitone phasecal mode in *fourfit*. The difference is that, although the multitone phasecal mode does use all the tones in a band to calculate a band-wide delay, that delay is not stored as a quantity in the *fourfit* output. It is used only in the *fourfit* processing to calculate the phase for the multitone delay at the mean frequency of each channel and the difference of that phase to the actual phasecal phase at that frequency. The difference is applied as a correction to the cross-correlation phase.

The primary cause for phase variation within the signal chain is temperature change of the components and of the connecting cables, and the main driver for this is the air conditioning (AC, taken to include both heating and cooling). The proxy cable delay measurements for GGAO12M for 2022 May 19 are shown in Figure 3. Although no temperature measurements in the area of the signal chain were being made at this time, the temperatures in the electronics racks and control room were measured in the past and showed very similar characteristics. In particular, the interval between cycles is correlated with the outside temperature as would be expected. The time-scale for the changes in phase is thus tied to the heating and cooling provided by the AC, which typically should have a cycle time of tens of minutes or more. These affect the pcmt delays but not to measurements by the CDMS. Similarly, the delay in the reference-frequency cable is dependent on the external temperature and on direct solar illumination, moderated by the thermal inertia of the cables. The combined effects also should have a time-scale of tens of minutes or more, and they are present in both the CDMS and the pcmt delay.

In contrast, the changes in antenna orientation during a VGOS observing session that may affect the reference-frequency cable delay occur in less than a minute because of the rapid source-switching of the VGOS schedules. This difference in timescales can be used to separate the orientation-dependent delay ‘errors’ from the longer-timescale thermal variations by using some form of temporal smoothing with a characteristic time that is long compared to that of the orientation-dependent errors but short enough to respond to the thermal variations. Such temporal smoothing is provided in the geodetic estimation process by the piecewise-linear (PWL) models that are used for the clock delays.

While the paths through the signal chain electronics vary from frequency to frequency due to the different electrical components (amplifiers, frequency converters, filters, cables, etc), the path from the H-maser to the phasecal generator is common to all frequencies. In principle, then, the temporal changes in proxy cablecal delay from any one band and polarization could provide the variation of the cable with time. However, since the pcmt delays occasionally differ among these eight paths (four bands and two polarizations) due to different instrumentation and cables, the pcmt delay is, in practice, calculated for all eight paths for comparison. For several antennas the RF down-link cables for Band A are of a different type from Bands B-D (for example, coax instead of optical fiber for the NASA and AUSCOPE antennas), resulting in significantly different temporal behavior. As a consequence, the default is to average the pcmt delays of both polarizations of Bands B-D for each scan and to use these average values for the final proxy cablecal delay measurements.

So, in summary, 1) the use of the multitone phasecal in *fourfit* aligns the phases within each band for maximum coherence; and 2) application of the pcmt delay in the post-*fourfit* analysis (e.g. *nuSolve)* subtracts the orientation-dependent and other delays due to the reference cable, as well as re-introducing the signal chain variations which are absorbed in the estimated clock parameters.

3. Modeling the cable delay temporal variations

To evaluate the effect of (mis-)modeling those factors that affect the proxy cablecal delays (for example temperature changes of the signal chain components), the pcmt values have been modeled as observables that result from the combined effects of a time-varying clock, an error in the *a priori* position of one antenna, and atmosphere ZWD and gradient. The model consists of a continuous piecewise-linear function with fixed time intervals for the temporal dependence of the clock, plus the delay due to the offset of the antenna position expressed in local East, North, and Up (ENU) coordinates, plus one value for the ZWD and two for the gradient for the full session. (Azimuth is measured towards East from North.) The model and estimation calculations are described in Appendix A.1 and implemented in a *matlab* script described in Appendix A.3:

```
c:\aa\IVS\VGOS\VR\vr2203\cablecal_CZG_pwl_fit_GGAO.m     (clock, position, ZWD, and gradient)
```

An uncertainty of 2 ps was assumed for each delay value for the weighted least-squares estimation. An iterative procedure was followed to increase an additive delay noise until the reduced chi-squared has a value of 1.0 within a tolerance of 0.1. (See Appendix A.2 for details.)

In the script it is also possible to introduce an *apriori* position offset in order to see how reliably the offset is recovered in the presence of the cablecal variations.

4. Application to GGAO12M

GGAO12M is one of the VGOS antennas that does not have a hardware cable delay calibration system. Others are ISHIOKA and the AUSCOPE antennas. Two antennas have a CDMS but the data have not been available: KOKEE12M and MACGO12M. (The RAEGEYEB CDMS system has been questionable or unusable at times, as has WETTZ13S. The phasecal systems for these antennas have generally worked well enough that the proxy cablecal could be utilized, although there were periods for RAEGEYEB and ISHIOKA when this was not true. For RAEGEYEB the apparent failure of the CDMS and phasecal may both have on occasion been due to a defective reference frequency cable.)

GGAO12M is the prototype VGOS antenna, and the limitation of not having a CDMS was realized early in its usage (see Niell et al 2018). As a consequence, the orientation dependence of the cable delay has been monitored approximately monthly since 2016. Examples of that dependence are seen in Figures 1, 2, and 4.

The data used for evaluation of the clock/position/atmosphere error model are from three VGOS sessions (Table 1).

Session	vgosDb	Correlator	expt number
vr2203	22MAY19VG	Haystack	3811
vo2195	22JUL14VG	TUVien	5329
vt7017	17JAN17VG	Haystack	3585

The session vr2203 was selected for two reasons: a) by design it has a larger number of scans than the vo sessions observed to date, and b) the az-el dependence of the proxy cablecal delay for GGAO12M was measured approximately one month before and showed very small (less than 5 ps) variation in the median values of both azimuth and elevation (Figure 1). Session vo2195 was selected because the az-el measurements for GGAO12M were obtained only two days before and had a large variation (approximately 40 ps peak to peak) in azimuth but small variation (less than 3 ps) in elevation. Session vt7017 was analyzed because it exhibited, among the first two years of GGAO12M-WESTFORD sessions, the largest baseline length discrepancy for when the GGAO12M proxy cablecal was not applied (Niell et al 2018). (Since that session the variation of the reference frequency cable delay with azimuth and elevation (called the 'az-el measurements') has been monitored approximately monthly to look for increasing variations, and the 5-MHz cable has been replaced before the variations became as large as was seen in vt7017.) These sessions provide evidence that the proxy cablecal can serve as a satisfactory, but less precise, backup for the missing cable delay measurement system for GGAO12M.

It is reasonable to ask what the minimum length of the PWL interval for the clock should be to determine the parameters that are being estimated for that interval. In a complete geodetic analysis, in addition to the clock values at the ends of the interval, a zenith wet delay (ZWD) and two atmosphere gradient parameters are also estimated as PWL. The interval for the ZWD may be comparable to that of the clock, and, while the gradient parameter interval is usually longer, some investigations have concluded that those intervals should also be short. To evaluate the minimum PWL interval (but not used in the calculations below) I will assume that the ZWD and gradients and their rates are also being estimated with the same clock interval. For that case the total number of parameters is four after the first interval (the end point values for each parameter). For this the minimum number of observations per interval needed for the parameters to be slightly overdetermined is five. The interval needed to obtain this number of observations can be calculated from the total number of observations at an antenna over the length of the session (t_min = 1440 min * 5 obs per seg / N_obs). For the three sessions described in the preceding paragraph the minimum interval lengths, based on this calculation, would range from five to seven minutes. This is a lower limit to the PWL interval from a statistical point and is likely to be smaller than the minimum interval required by any other consideration.

4.1 Results of estimating clocks, station position, ZWD, and atmosphere delay gradients

For testing with the model of Section 3, the length of the PWL interval was varied from 60 minutes down to 2 minutes to determine a) how the WRMS of the post-fit cablecal delay values changed with PWL interval, and b) how the estimated position changed with PWL interval. The shortest intervals were included to investigate what length interval is needed to capture the rapid variations of the cablecal delay.

The estimation script was run first on the three sessions described above with no *a priori* offset for the position. The results are given in Table 1.

Table 1. Summary of results for estimating a piecewise linear clock, the ENU coordinates of the antenna, ZWD, and atmosphere gradient for a range of PWL intervals (*PWLint* in minutes). The units for added noise (*nois*)and *WRMS* are picoseconds. *c2rAB* is the reduced chi-squared after reweighting. The units for ENU, ZWD, and atmosphere delay gradient components and their uncertainties are millimeters.

1a. Summary for offset = 0 for vr2203 (N_obs = 1550):

PWLint	nois	WRMS	c2rAB	off	az	E	N	U	ZWD	Ge	Gn
60.0	15.4	15.6	1.0	0.0	0.0	-0.7	-0.4	0.9	-0.4	-0.1	0.0
		uncertainty(chi2r=1)				0.5	0.6	1.0	0.5	0.6	1.0
30.0	15.5	15.5	1.0	0.0	0.0	-0.7	-0.4	1.0	-0.5	-0.1	-0.0
		uncertainty(chi2r=1)				0.5	0.6	1.0	0.5	0.6	1.0
15.0	14.5	13.9	1.0	0.0	0.0	-0.8	-0.3	0.6	-0.4	-0.0	-0.0
		uncertainty(chi2r=1)				0.5	0.6	0.9	0.5	0.6	0.9
10.0	10.7	10.8	1.1	0.0	0.0	-1.0	-0.1	0.6	-0.4	0.0	-0.0
		uncertainty(chi2r=1)				0.3	0.4	0.7	0.3	0.4	0.7
5.0	4.2	4.4	1.1	0.0	0.0	-1.0	-0.6	0.4	-0.2	0.0	0.1
		uncertainty(chi2r=1)				0.2	0.2	0.3	0.2	0.2	0.3
3.0	2.0	2.4	1.0	0.0	0.0	-1.2	-0.3	0.4	-0.2	0.1	0.0
		uncertainty(chi2r=1)				0.1	0.1	0.2	0.1	0.1	0.2
2.0	0.7	1.6	1.1	0.0	0.0	-1.1	-0.4	0.1	-0.2	0.1	0.0
		uncertainty(chi2r=1)				0.1	0.1	0.2	0.1	0.1	0.2

1b. Summary for offset = 0 for vo2195 (N_obs = 1179):

PWLint	nois	WRMS	c2rAB	off	az	E	N	U	ZWD	Ge	Gn
60.0	12.5	12.5	1.0	0.0	0.0	-3.2	-0.4	0.3	-0.4	0.0	-0.1
		uncertainty(chi2r=1)				0.5	0.5	1.0	0.5	0.5	1.0
30.0	12.5	12.4	1.0	0.0	0.0	-3.1	-0.3	0.3	-0.4	0.0	-0.1
		uncertainty(chi2r=1)				0.5	0.5	1.0	0.5	0.5	1.0
15.0	12.4	11.9	1.0	0.0	0.0	-2.7	-0.4	0.1	-0.3	-0.1	-0.1
		uncertainty(chi2r=1)				0.5	0.5	1.0	0.5	0.5	1.0
10.0	10.1	9.6	1.0	0.0	0.0	-3.1	-0.7	0.6	-0.3	0.1	0.0
		uncertainty(chi2r=1)				0.4	0.5	0.8	0.4	0.5	0.8
5.0	6.1	5.4	1.0	0.0	0.0	-3.0	-0.9	0.1	-0.3	0.1	0.0
		uncertainty(chi2r=1)				0.3	0.3	0.5	0.3	0.3	0.5
3.0	5.1	4.0	1.0	0.0	0.0	-2.6	-1.1	-0.1	-0.2	0.0	0.1
		uncertainty(chi2r=1)				0.3	0.3	0.5	0.3	0.3	0.5
2.0	4.9	2.8	1.0	0.0	0.0	-2.7	-1.1	-0.7	-0.2	0.1	0.1
		uncertainty(chi2r=1)				0.3	0.4	0.7	0.3	0.4	0.7

1c. Summary for offset = 0 for vt7017 (N_obs = 1179):

PWLint	nois	WRMS	c2rAB	off	az	E	N	U	ZWD	Ge	Gn
60.0	36.7	37.6	1.1	0.0	0.0	-7.4	-14.1	-2.0	0.1	0.6	0.9
		uncertainty(chi2r=1)				1.4	1.5	2.8	1.4	1.5	2.8
30.0	34.7	34.0	1.0	0.0	0.0	-7.1	-13.6	-2.5	0.3	0.6	1.0
		uncertainty(chi2r=1)				1.4	1.5	2.6	1.4	1.5	2.6
15.0	28.4	27.4	1.0	0.0	0.0	-6.8	-11.2	-2.7	0.4	0.7	0.9
		uncertainty(chi2r=1)				1.1	1.2	2.2	1.1	1.2	2.2
10.0	26.7	24.6	1.0	0.0	0.0	-4.8	-10.5	-1.0	0.4	0.3	0.7
		uncertainty(chi2r=1)				1.1	1.2	2.1	1.1	1.2	2.1
5.0	23.0	20.0	1.0	0.0	0.0	-2.9	-9.6	-0.8	0.1	0.2	0.6
		uncertainty(chi2r=1)				1.1	1.2	1.9	1.1	1.2	1.9
3.0	20.1	16.2	1.1	0.0	0.0	-1.9	-9.6	-0.5	0.2	0.3	0.7
		uncertainty(chi2r=1)				1.1	1.1	1.9	1.1	1.1	1.9
2.0	19.1	12.0	1.0	0.0	0.0	-1.0	-11.1	0.3	0.3	0.2	0.7
		uncertainty(chi2r=1)				1.2	1.3	2.1	1.2	1.3	2.1

The first thing to observe in these results is the reduction in the amount of added noise needed to achieve chi-squared ~ 1 as the PWL interval decreases. This is a consequence of the PWL interval becoming shorter than the time scale of the temporal variations and thus approximating the time variation more closely.

It is important to note that if a cable delay measurement system were operating, the cable delay variations would be removed without adding the temporal variations from the signal chain, which artificially increases the WRMS and thus the position uncertainties.

The cablecal delays for vr2203 and the estimated PWL fit for an interval of 60 minutes are shown in Figure 5 and for an interval of 5 minutes in Figure 6. The corresponding post-fit delay residuals are shown in Figure 7.

Since there is no CDMS for GGAO12M, it is important to set the interval for the PWL model as short as possible to avoid adding unnecessary delay noise to the geodetic solution. Unfortunately, since many (perhaps all) geodetic analysis packages allow only one interval to be set for all stations for each effect (clock, ZWD, and atmosphere delay gradient), a shorter interval for the other stations is required than would otherwise be used. This can increase the parameter estimate uncertainties, by adding unnecessary parameters, if such short intervals were otherwise not needed.

A second thing that can be learned from this exercise is that the effect of the cable delay variation with orientation on the position estimate for the observed session delays can be derived from the pcmt values for that session. For the more recent of the three sessions (vr2203 and vo2195) the estimated offsets in ENU vary by less than 0.5 mm about the average offset as the PWL interval is varied from 5 minutes to 60 minutes, suggesting that the actual position errors are insensitive to the PWL interval.

For vr2203 the estimated position offset is less than 1 mm (within one sigma) in all ENU components for a PWL interval of 10 minutes are less. This is consistent with the delays seen in the az-el measurements of 22 Apr 11 (Figure 1) for which the largest delay is approximately 2 ps.

For vo2195 the estimated position offset is approximately 3 mm in the East component, which is consistent with delays for the az-el measurements of 22 Jul 14 (Figure 2): 20 ps peak-to-peak is approximately a 10 ps amplitude which corresponds to ~3mm displacement.

The minimum WRMS for vt7017 is much larger than for the two other sessions. This might be expected, given the large variation of the elevation-dependent delays, from ~15 ps peak-to-peak at low elevations to ~40 ps above 30°, as seen in the right panel of Figure 4. The peak-to-peak value of 40 ps corresponds to an RMS of about 10 ps. Although it is consistent with the value of 12 ps found for the shortest PWL interval in Table 1c, this convenient explanation is probably not correct since, if the large variations in elevation were due to the 5-MHz cable, the pcmt should have corrected them. Another candidate for the additional scatter is variation in the signal chain, since this would be added back in with application of the pcmt. However, this is argued against by the fact that application of the pcmt reduces the WRMS of the post-fit delay residuals in nuSolve by a significant amount compared to no pcmt. This issue is unresolved.

The scatter and systematic variation in the azimuth and elevation delay errors, as seen in the az-el measurements, began to increase in late 2016, reaching the extent show in Figure 4, just before vt7017. The 5-MHz cable was replaced shortly after this and the orientation-dependent variation disappeared, reappearing only as the replacement cable degraded due to the antenna motion.

4.2 Comparison of pcmt position offset with offset estimated from *nuSolve* for vt7017

If the dependence of the pcmt delay on position error has been modeled correctly, the estimated position offset for the *pcmt* observables should agree with the difference in position estimated by *nuSolve* between using (*pcmt*) and not using (*NOpcmt*) the pcmt correction to the delays.

The corresponding *nuSolve* estimates are given in the following two solutions.

```
17JAN17VG_C20Z15G6_GsNOpcmt.SFF:       GGAO12M  7622       U Comp              16.34
mm         16.338 mm              3.300 mm              2.880 mm
17JAN17VG_C20Z15G6_GsNOpcmt.SFF:       GGAO12M  7622       E Comp               5.71
mm          5.713 mm              0.848 mm              0.740 mm
17JAN17VG_C20Z15G6_GsNOpcmt.SFF:       GGAO12M  7622       N Comp              16.40
mm         16.397 mm              0.901 mm              0.786 mm

17JAN17VG_C20Z15G6_Gspcmt.SFF:         GGAO12M  7622       U Comp               7.96
mm          7.956 mm              2.444 mm              1.978 mm
17JAN17VG_C20Z15G6_Gspcmt.SFF:         GGAO12M  7622       E Comp              -1.81
mm         -1.808 mm              0.618 mm              0.500 mm
17JAN17VG_C20Z15G6_Gspcmt.SFF:         GGAO12M  7622       N Comp               3.24
mm          3.244 mm              0.660 mm              0.534 mm
```

In the following table the difference of these solutions is compared with the position offset estimated from the pcmt data. The averages of the offsets for the PWL intervals of 15 min and 30 min are used since the *nuSolve* solution was for a 20-minute clock interval.

	nuSolve	pcmt	pcmt-nuSolve
comp	pcmt minus NOpcmt	PWLENU (30min/15min avg)	PWLENU minus nuSolve
E	-7.5 (0.8) mm	-7.0 (1.3) mm	0.5 mm
N	-13.2 (0.9) mm	-12.4 (1.4) mm	0.8 mm
U	-8.4 (3.3) mm	-2.6 (2.4) mm	5.8 mm

Thus, the position correction estimated from the pcmt measurements agrees with the actual change in horizontal position to a millimeter when the pcmt delays are applied in the geodetic estimation, while the Up component differs by six millimeters. The latter is an approximately two sigma difference.

So all three sessions indicate that the pcmt delays provide a cablecal correction good to 1 mm in the horizontal and better than 6 mm in Up. The accuracy of the horizontal correction is further supported by the application to GGAO12M and WESTFORD as discussed in Niell et al (2018) when application of the proxy cablecal reduced the deviation of the baseline length from the mean for 14 of the 19 sessions, resulting in a WRMS of the lengths of only 1.6 mm.

5. Summary

The phase calibration system is used primarily to correct for the different phase and delay contributions experienced by the many VGOS signal channels so they may be combined coherently. In addition, all of the signal channels experience a common delay due to the cable that conveys the reference frequency from its origin to the phasecal generator. In a fully implemented VGOS system this delay is measured by the cable delay measurement system (CDMS). Thus, for the standard VGOS station configuration, the phasecal corrections are applied as part of the correlation process, and the common delay of the reference frequency cable is removed in the geodetic estimation process by applying the CDMS measurement for each observation.

The main value of the CDMS is to obtain measurements of any orientation-dependent deviations of the cable delays. If left uncorrected, these azimuth- and elevation-dependent delay errors will result in anomalous position errors.

For those VGOS stations that have not implemented a CDMS, or for which the CDMS is not functioning, a proxy has been found. Since the phasecal tones experience the entire delay from the reference frequency generation point to the formatter, they are affected by the deformations of the reference frequency cable. Thus, the group delay formed by the phase vs frequency of the phasecal tones within a band (the multitone phasecal delay, or pcmt delay) provides that round trip delay. An average among all bands will reduce the band-dependent differences while preserving the common-delay signature, including the orientation-dependent delays. Common-band delay variations also result from temperature changes in the signal chain path from the phasecal injection point to the formatter.

For the pcmt delay to be useful as a proxy for the CDMS for the orientation-dependent (az-el) errors, it must be possible to separate the pcmt delay variations due to the orientation variations from the signal chain part of the variations in the pcmt delays. It is possible to make this separation by virtue of the different time scales of the variations. The thermal variations in the signal chain components have a characteristic time scale generally of ten minutes or more, while the azimuth and elevation change significantly from scan to scan on a time scale of about one minute or less. Thus, modeling the clock as piecewise linear with an interval of ten minutes or more provides a baseline from which the azimuth- and elevation-dependent delay deviations can be measured.

Traditionally the PWL parameterization of the station clocks has been given an interval of 60 minutes. However, that value has been reduced for VGOS in light of the much higher precision and higher frequency of the group delay measurements within a session. Even so, the interval used for operational analysis is rarely less than 30 minutes. This is generally satisfactory when the phasecal has removed the signal chain variations and the CDMS has removed the cable delay variations. It is insufficiently short when there are large (tens of picoseconds) short-time-scale (twenty minutes) variations of the signal chain delay. These are present in the pcmt delays for GGAO12M and are due to rapid cycling of the air conditioning. As a consequence, using the pcmt delays as a proxy correction for the cable delays re-introduces these cyclical delay variations in the group delays. (The signal chain variations were removed by the application of the multitone phasecal in *fourfit*.) If a PWL interval comparable to, or longer than, the time scale of the cyclical variations is used, the scatter of the group delays will be increased. Reducing the interval will allow the modeled variations to more closely follow the cyclical variations. The challenge is to set the PWL interval short enough to fit these variations but long enough to provide a baseline for the az-el delay deviations.

The cyclical variations are very evident in the pcmt delays of GGAO12M, with peak to peak deviations up to 60 ps for the sessions in 2022. Two sessions in 2022, vr2203 (22MAY19VG) and vo2195 (22JUL14VG), were used to evaluate the added noise contribution to a geodetic solution when modeled as a continuous PWL clock, a position offset, and an atmosphere ZWD and gradient. Based on just these two sessions, the PWL interval should be kept to 10 minutes or less in order to require an added noise of 10 ps or less, while an interval of 30 minutes or greater will add 12 to 15 ps of noise. These are significant when compared to the median group delay uncertainty of ~2 ps for vr2203 and vo2195, but are not significant in the presence of the overall session WRMSs of greater than 30 ps. This large scatter is likely due to source structure, so until those delay contributions are mitigated, the PWL interval of the clock model is not so significant.

The expected effect of the pcmt delay correction on the geodetic results was evaluated by treating the pcmt values as observables and estimating the parameter adjustments for antenna position, the clock as a piecewise continuous linear function, and atmosphere ZWD and gradient. For two vgos sessions the resulting position estimates are consistent at the millimeter level with those expected based on delay variations in azimuth and elevation measured independently.

References

González-García, J.; Patino-Esteban, M.; Beltrán-Martínez, F.J.; Bautista-Durán, M.; López-Espí, P.L.; López-Pérez, J.A. New Cable Delay Measurement System for VGOS Stations. Sensors 2022, 22, 2308. https://doi.org/10.3390/s22062308

Niell A, Barrett J, Burns A, Cappallo R, Corey B, Derome M, Eckert C, Elosegui P, McWhirter R, Poirier M, Rajagopalan G, Rogers A, Ruszczyk C, SooHoo J, Titus M, Whitney A, Behrend D, Bolotin S, Gipson J, Gordon D, Himwich E, Petrachenko B (2018) Demonstration of a broadband very long baseline interferometer system: A new instrument for high-precision space geodesy. Radio Sci 53:1269–1291

Rogers. AEE (2020) https://www.haystack.mit.edu/wp-content/uploads/2020/07/memo_VGOS_023.pdf (digital picosecond comparator)

Ruszczyk et al (2023) The Haystack Cable Delay Measurement System (in preparation),

Vierinen, Juha, and Beaudoin, Christopher 2014, Low cost software radio picosecond phase comparator (SDR CDMS), memo 2014

Appendices

A.1 Linear least squares estimation of clocks, position, and atmosphere ZWD and gradient.

Equations for PWL fit for clock, position, ZWD, and atmosphere delay gradient to delay observations.

$$\tau_{obs} = \tau_{clk} + \tau_{posn} + \tau_{ZWD} + \tau_{grad} \tag{1}$$

τ_{obs} = N_{obs} by 1 column vector of the observations (in this case the proxy cablecal delays)

τ_{clk} = continuous piecewise linear model for the clock

τ_{posn}= dependence of delay on position offset from the assumed origin

τ_{ZWD} = continuous piecewise linear model for the zenith wet delay (ZWD)

τ_{grad}= continuous piecewise linear model for the atmosphere delay gradient

The PWL function can be represented either as an initial value and a series of rates for each segment, or as an initial value and a series of values at the end of each segment. I use the second one.

Let

i = the index of the observations, which are tagged by time t_i.
N_{clk} = number of clock segments
k = the index of the PWL segments, k= 1,N_{clk}
T_{PWL} = length of each segment
T_0 = the time at the beginning of the first segment
T_k = the time at the end of each segment for k = 1, N_{clk}
C_0 = the value of the clock parameter at the beginning of the first segment
C_k = value of the clock parameter at the end of each segments for k = 1, N_{clk}.

Then for an observation at time t_i in PWL interval k the clock is described by:

$$\begin{aligned}\tau_{clk}(t_i) &= C_0 + (C_1 - C_0) + \cdots + (C_k - C_{k-1}) + (C_{k+1} - C_k)\left\lfloor \frac{t_i - t_k}{T_{PWL}} \right\rfloor \\ &= C_k + (C_{k+1} - C_k)\left\lfloor \frac{t_i - t_k}{T_{PWL}} \right\rfloor \text{ for } t_k \le t_i < t_{k+1}\end{aligned} \tag{2}$$

Within each clock interval $T_k \le t_i < T_k$ the partial derives for the clock parameters are:

$$\begin{aligned}\frac{\partial \tau_{obs}(t_i)}{\partial C_k} &= 1 - \left\lfloor \frac{t_i - t_k}{T_{PWL}} \right\rfloor \\ \frac{\partial \tau_{obs}(t_i)}{\partial C_{k+1}} &= \left\lfloor \frac{t_i - t_k}{T_{PWL}} \right\rfloor\end{aligned} \tag{3}$$

For ZWD replace C by Z, although the number of segments is likely to be different.

The position offset is defined by East (E), North (N), and Up (U) coordinates relative to the origin for an observation at time t_i made at an azimuth of az_i and an elevation of el_i (both in radians). The

azimuth direction is measure East from North, so that a positive delay for an observation to the East would give an estimated position in the negative East direction. The delay is then given by:

$$\begin{aligned}\tau_{posn}(t_i) = \frac{1}{c}[&-E\cdot\sin(az(t_i))\cdot\cos(el(t_i))\\ &-N\cdot\cos(az(t_i))\cdot\cos(el(t_i))\\ &-U\cdot\sin(el(t_i))]\end{aligned} \tag{4}$$

The atmosphere gradient delay is expressed in components to the East and North, estimated as separate parameters, G_E and G_N. The mapping function that is usually used to modify the azimuth terms is approximated by 1/sin(el) for this simulation.

$$\tau_G(t_i) = -\frac{1}{\sin(el_i)}\cdot\left(G_E\cdot\sin(az_i) + G_N\cdot\cos(az_i)\right) \tag{5}$$

Since the observed delay is linear in all parameters, the values of the parameters can be estimated by weighted linear least squares.

C = clock partials [N_{obs} x (N_{clk}+1)]

$$C = \begin{bmatrix}
1-\left[\frac{t_i-T_0}{T_{PWL}}\right] & \left[\frac{t_i-T_0}{T_{PWL}}\right] & 0 & 0 & \cdots & 0 & 0 \\
\vdots & & & & & & \\
1-\left[\frac{t_i-T_0}{T_{PWL}}\right] & \left[\frac{t_i-T_0}{T_{PWL}}\right] & 0 & 0 & \cdots & 0 & 0 \\
0 & 1-\left[\frac{t_i-T_1}{T_{PWL}}\right] & \left[\frac{t_i-T_1}{T_{PWL}}\right] & 0 & \cdots & 0 & 0 \\
\vdots & & & & & & \\
0 & 1-\left[\frac{t_i-T_1}{T_{PWL}}\right] & \left[\frac{t_i-T_1}{T_{PWL}}\right] & 0 & \cdots & 0 & 0 \\
\vdots & & & & & & \\
\vdots & & & & & & \\
0 & 0 & 0 & 0 & \cdots & 1-\left[\frac{t_i-T_{Nclk}}{T_{PWL}}\right] & \left[\frac{t_i-T_{Nclk}}{T_{PWL}}\right] \\
\vdots & & & & & & \\
0 & 0 & 0 & 0 & \cdots & 1-\left[\frac{t_i-T_{Nclk}}{T_{PWL}}\right] & \left[\frac{t_i-T_{Nclk}}{T_{PWL}}\right]
\end{bmatrix} \tag{6}$$

B = ZWD partials [N_{obs} x (N_{ZWD}+1)]

same as for clock but $T_{clk} \rightarrow T_{ZWD}$

P = ENU partials [N_{obs} x 3]

$$P = \begin{bmatrix} -\sin(az(t_1))\cos(el(t_1)) & -\cos(az(t_1))\cos(el(t_1)) & -\cos(el(t_1)) \\ \vdots & & \\ -\sin(az(t_{Nobs}))\cos(el(t_{Nobs})) & -\cos(az(t_{Nobs}))\cos(el(t_{Nobs})) & -\cos(el(t_{Nobs})) \end{bmatrix} \quad (7)$$

G = gradient partials [N_{obs} x 2]

$$P = \begin{bmatrix} -\sin(az(t_1))\cos(el(t_1))/\sin(el(t_1)) & -\cos(az(t_1))\cos(el(t_1))/\sin(el(t_1)) \\ \vdots & \\ -\sin(az(t_1))\cos(el(t_1))/\sin(el(t_1)) & -\cos(az(t_1))\cos(el(t_1))/\sin(el(t_1)) \end{bmatrix} \quad (8)$$

X = unknowns [((N_{clk}+1) + (N_{ZWD}+1) + 3 +2) x 1]

A = all partials = [C | B | P | G] (i.e. the concatenation of individual arrays.

For uncertainty σ_i for each observation, the initial weight matrix, W, has only elements on the diagonal of value σ_i^{-2}.

The solution for the unknowns is given by:

$$X = (A^T W A)^{-1} A^T W \tau_{obs} \quad (9)$$

A.2 Re-weighting PWL LSQ for reduced chi-squared (chi2r) = 1.

$$chi2r = \sum_i \left(\frac{fit_i - obs_i}{\sigma_{obs,i}} \right)^2 * \frac{1}{(nobs - nparm)}$$

But $\sigma_{obs,i}$ is composed of the observation uncertainty and the added noise, each of which have only one value in this case, so it is common to all observations and can be taken out of the summation:

$$\sigma_{obs,i}{}^2 = \sigma_0{}^2 + noise^2 = \sigma_{obs}{}^2$$

$$chi2r = (\sigma_0{}^2 + noise^2)^{-1} \sum_i (fit_i - obs_i)^2 * \frac{1}{(nobs - nparm)}$$

then taking the derivative with respect to $noise^2$:

$$\frac{\partial chi2r}{\partial noise^2} = \frac{-1}{(\sigma_0{}^2 + noise^2)^2} * \sum_i (fit_i - obs_i)^2 * \frac{1}{(nobs - nparm)}$$

$$\frac{\partial chi2r}{\partial noise^2} = \frac{-1}{\sigma_0{}^2 + noise^2} * chi2r$$

So, to determine a first-order correction to noise2 for a value of chi2r greater than 1.0:

$$\Delta noise^2 = -\frac{\sigma_0{}^2 + noise^2}{chi2r} * (1.0 - chi2r)$$

For processing, set the tolerance to 0.1 and the fraction of the chi2r difference from 1.0 to 0.05.

The value of chi2r as noise increases is shown in Figure 8 for PWL = 5 minutes.

A.3 Fitting PWL to cablecal data.

cd c:\aa\IVS\VGOS\VR\vr2203

Estimate PWL clock for GGAO12M proxy cablecal using *matlab* script.

Modify c:\aa\Ivs\vlbi2010\gv12\2013May_FAC(fringe_amp_calib)\Sc_calibration\pwl_fit.m

-> `c:\aa\IVS\VGOS\VR\vr2203\cablecal_pwl_fit_GGAO`

Data are not equally spaced in time.

Use fixed-width time bins.

Model the cablecal delay as the value at 18:00 plus linear interpolation to next node at each bin-width in time.

i.e. ck = [ck(0); ck(1:n_bins,1)]

For LSQ fit, should input the uncertainty of the pcmt delay.

How can apriori uncertainty be obtained?

At the minimum, calculate the uncertainty from the fit of delay to the pc phases for a scan.

Extract the phasecal phases from a fourfit output for one or more bands.

Fit phases for linear phase(frequency) for each band: slope is the multitone delay.

This is what pcc_generate.py does: does it give quality of fit?

For now, estimate uncertainty as 2 ps. This will be adjusted by chi2r reweighting.

For both vr2203 and vo2195:

`for azimuth variation with amplitude =0 and 10 mm`

for `PWL_int_min =  60, 30, 15, 10, 6, 5, 3, 2 minutes`

estimate ENU coordinates

use additive noise to adjust chi2r

find eigenvalues/uncertainties of direction (extract from *\aa\DOTM\covar_trans.m*)

[V,D] = eig(cov_ENU);

Give and interpret the eigenvector and eigenvalues of the uncertainty ellipsoid (covariance).

To find the effect on baseline length of the error in position caused by the azel dependence of the cable delay, calculate the dot product of the position error (with no *a priori* offset) and the baseline vector.

To find the uncertainty in baseline length due to the cable delay position error, calculate the dot product of the baseline and the eigenvectors of the position offset covariance.

Figures

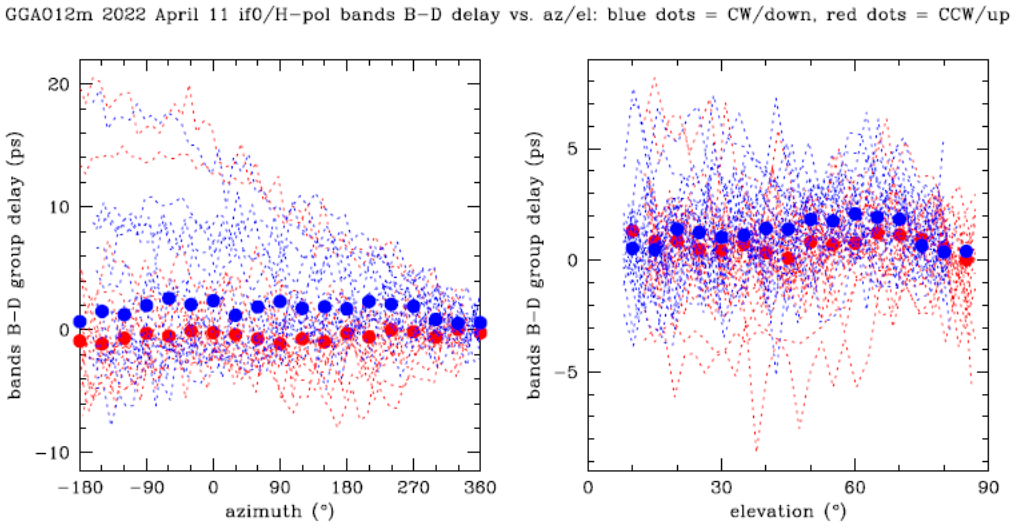

Figure 1. GGAO12M cabledelay az-el measurements 22 Apr 11 (38 days before vr2203) (*\aa\Ivs\VGOS\VR\vr2203\22Apr11_pcal_az-el_Gs_B-Dgroup.png*)

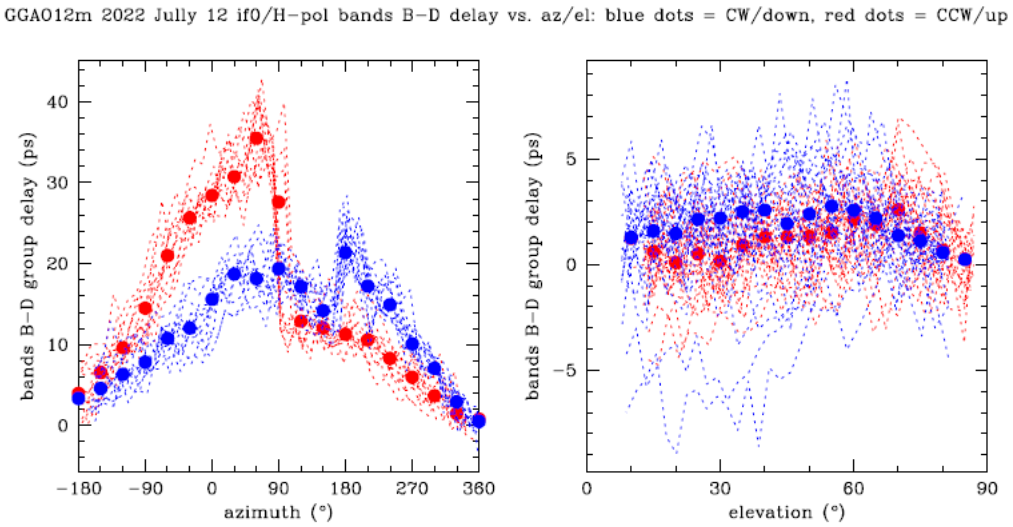

Figure 2. GGAO12M cabledelay az-el measurements 22 July 12 (two days before vo2195). The dots are the median values in 5° bins. (*\aa\Ivs\VGOS\VR\vr2203\22July12_pcal_azel_Gs_B-Dgroup.png*)

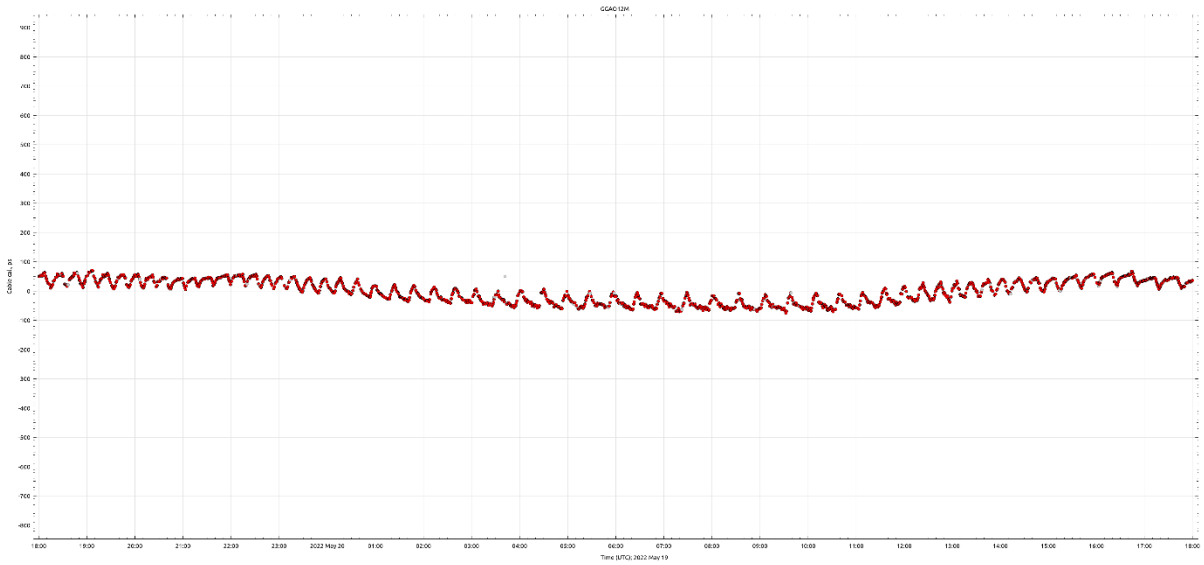

Figure 3. GGAO12M proxy cable delay measurements 22 May 19 (vr2203) (*\aa\Ivs\VGOS\VR\vr2203\22MAY19VG_Gs_cable.png:snipped from nuSolve station(plot) tab*)

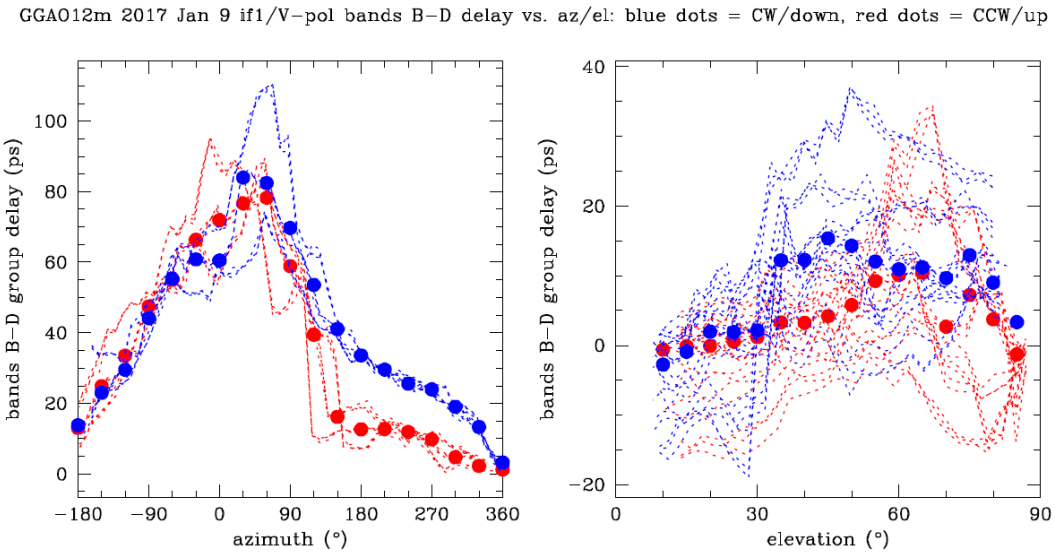

Figure 4. GGAO12M cabledelay az-el measurements 2017 Jan 9 (teight days before vt7017). The dots are the median values in 5° bins. (*\aa\Ivs\VGOS\VR\vr2203\17Jan17_pcal_azel_Gs_B-Dgroup.png*)

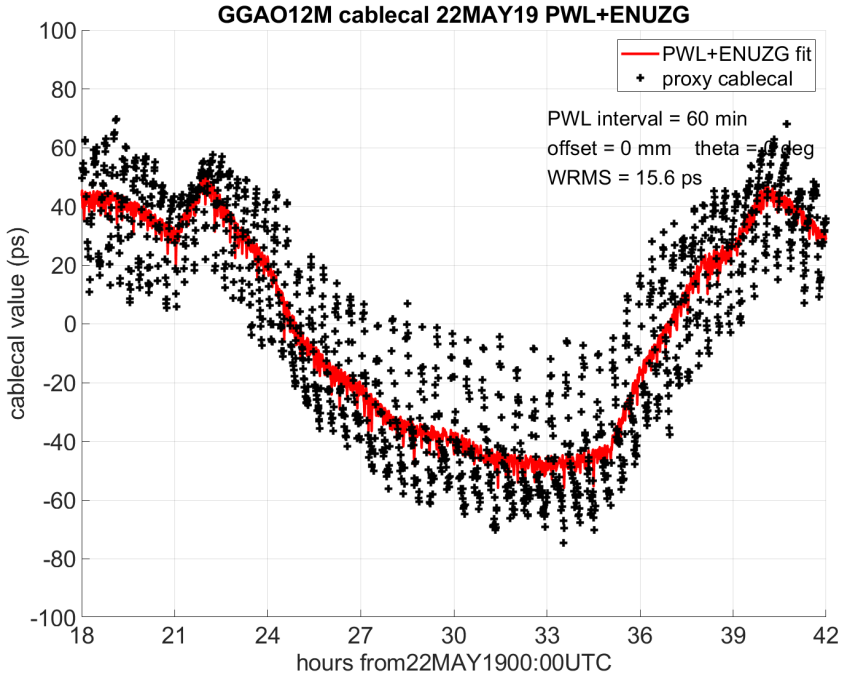

Figure 5. The observed cablecal delays for vr2203 (black cross) and the fitted values (red line) for estimated parameters for PWL clock with an interval of 60 minutes, ZWD, and atmosphere delay gradients. (*\aa\Ivs\VGOS\VR\vr2203\vr2203 0mm offset\vr2203 GGAO cablecal PWLENUZG 60min.PNG*)

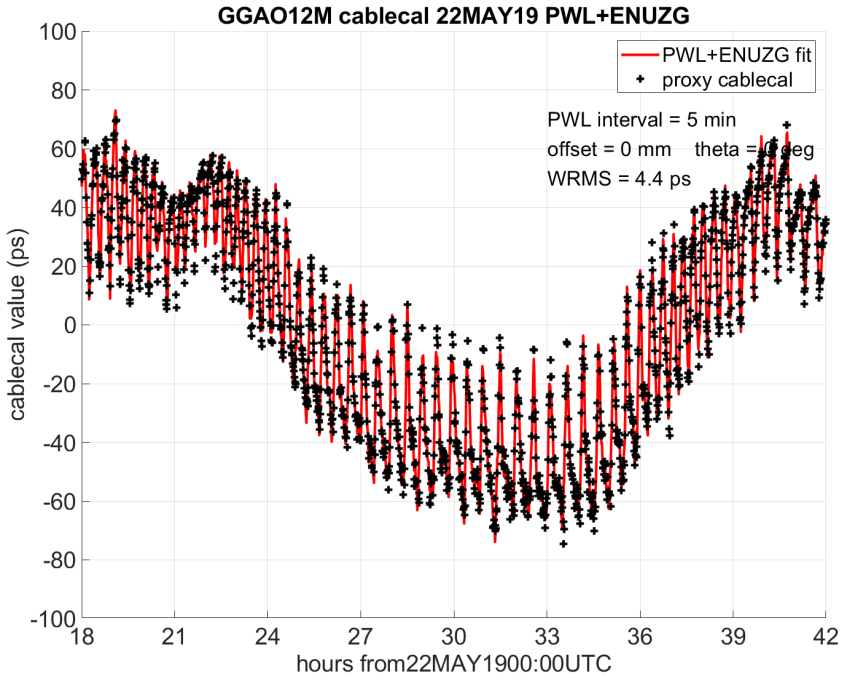

Figure 6. The observed cablecal delays for vr2203 (black cross) and the fitted values (red line) for estimated parameters for PWL clock with an interval of 5 minutes, ZWD, and atmosphere delay gradients. (*\aa\Ivs\VGOS\VR\vr2203\vr2203_0mm_offset\vr2203_GGAO_cablecal_PWLENUZG_5min.PNG*)

`

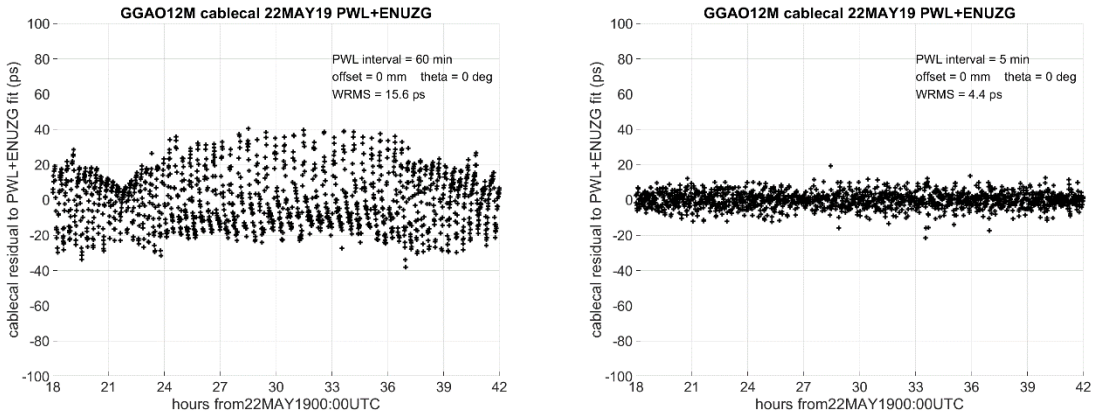

Figure 7. Post-fit delay residuals for vr2203 for PWL intervals of 60 minutes (left) and 5 minutes (right).
(*\aa\Ivs\VGOS\VR\vr2203\vr2203_0mm_offset\vr2203_GGAO_cablecal_PWLENUZG_pfdr_60min.PNG*) and *vr2203_GGAO_cablecal_PWLENUZG_pfdr_5min.PNG.*

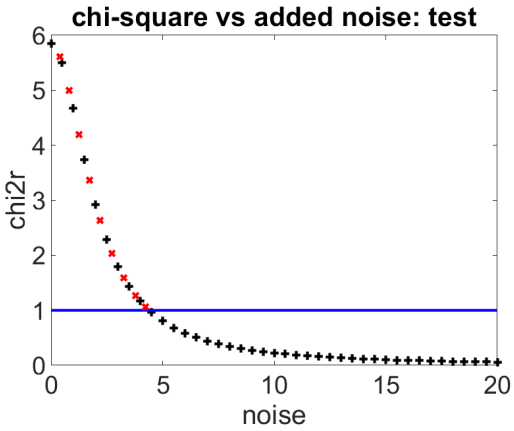

Figure 8. The value of chi2r as added noise increases for PWL = 5 minutes. x-axis is added noise in ps. black: value from data; red: steps in estimation process.
(\aa\Ivs\VGOS\VR\vr2203\vr2203_0mm_offset\vr2203_GGAO_cablecal_PWLENUZG_chi2r_noise_5min.png)